Electronic Supplementary Material (ESI) for Physical Chemistry Chemical Physics.
This journal is © the Owner Societies 2022

ELECTRONIC SUPPORTING INFORMATION (ESI) for

Single Level Tunneling Model for Molecular Junctions: Evaluating the Simulation Methods

Esther Martine, [a] Xianneng Song, [a] Xi Yu [a*] and Wenping Hu [a]

[a] *Tianjin Key Laboratory of Molecular Optoelectronic Science, School of Science, Tianjin University & Collaborative Innovation Center of Chemical Science and Engineering, Tianjin 300072, China.*

[*] *To whom correspondence should be addressed to Orcid.org/0000-0001-57507003; Email: xi.yu@tju.edu.cn*

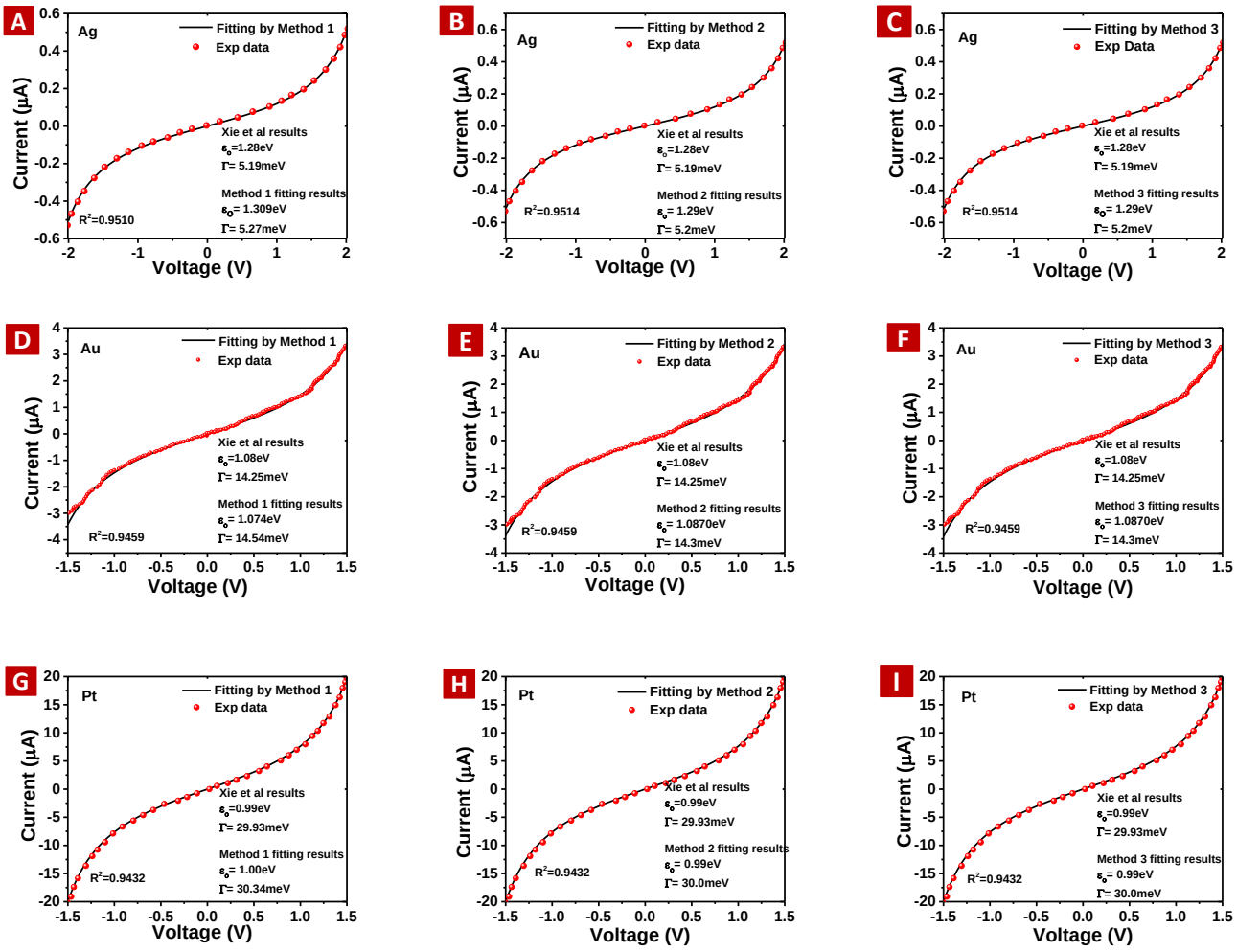

Fig S1: Current-Voltage plots and fitting of alkyl Dithiols, C8DT on Ag, Au, and Pt[1]

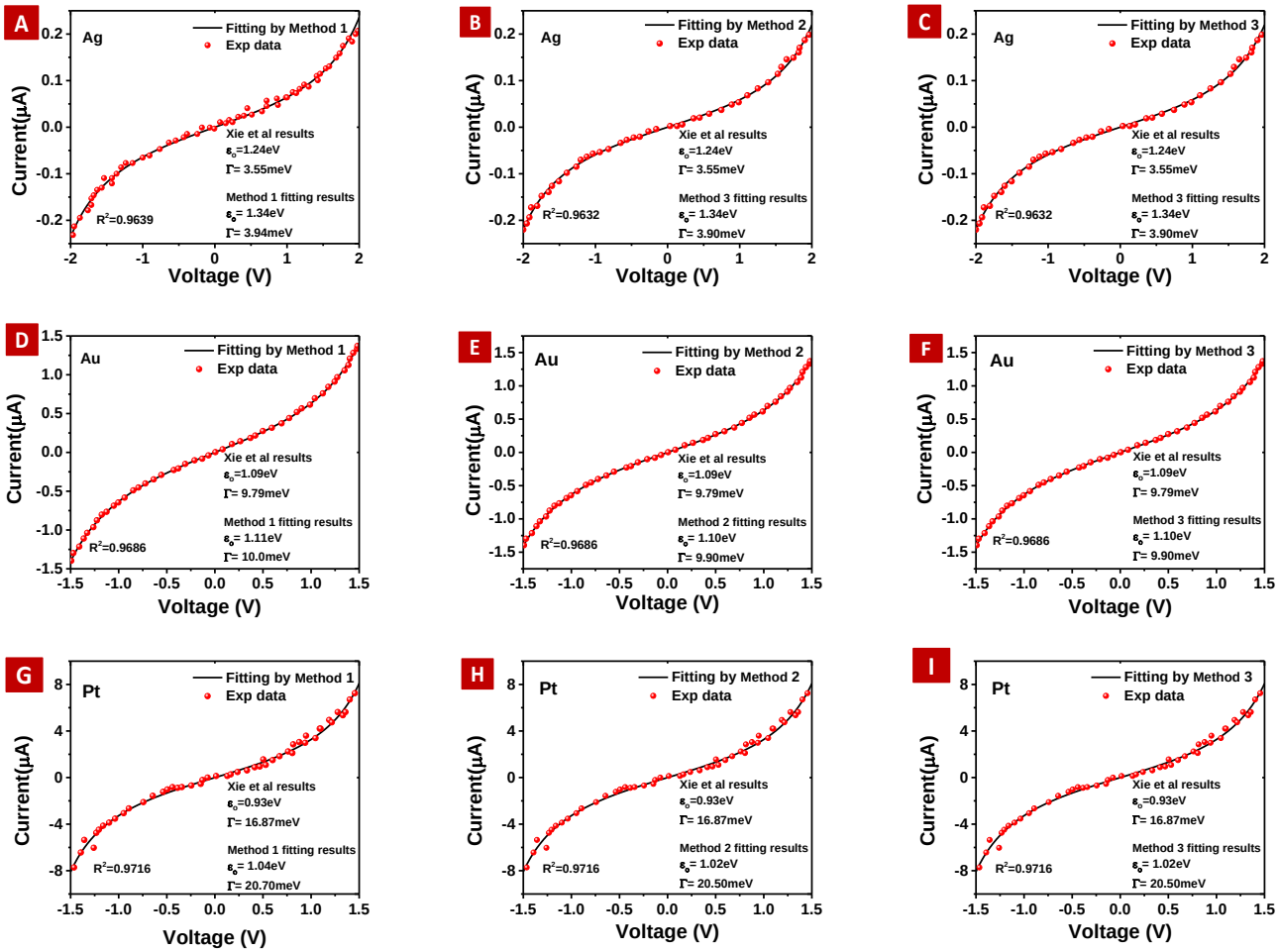

Fig S2: Current-Voltage Fitting plots of alkyl Dithiols, C9DT on Ag, Au, and Pt[1]

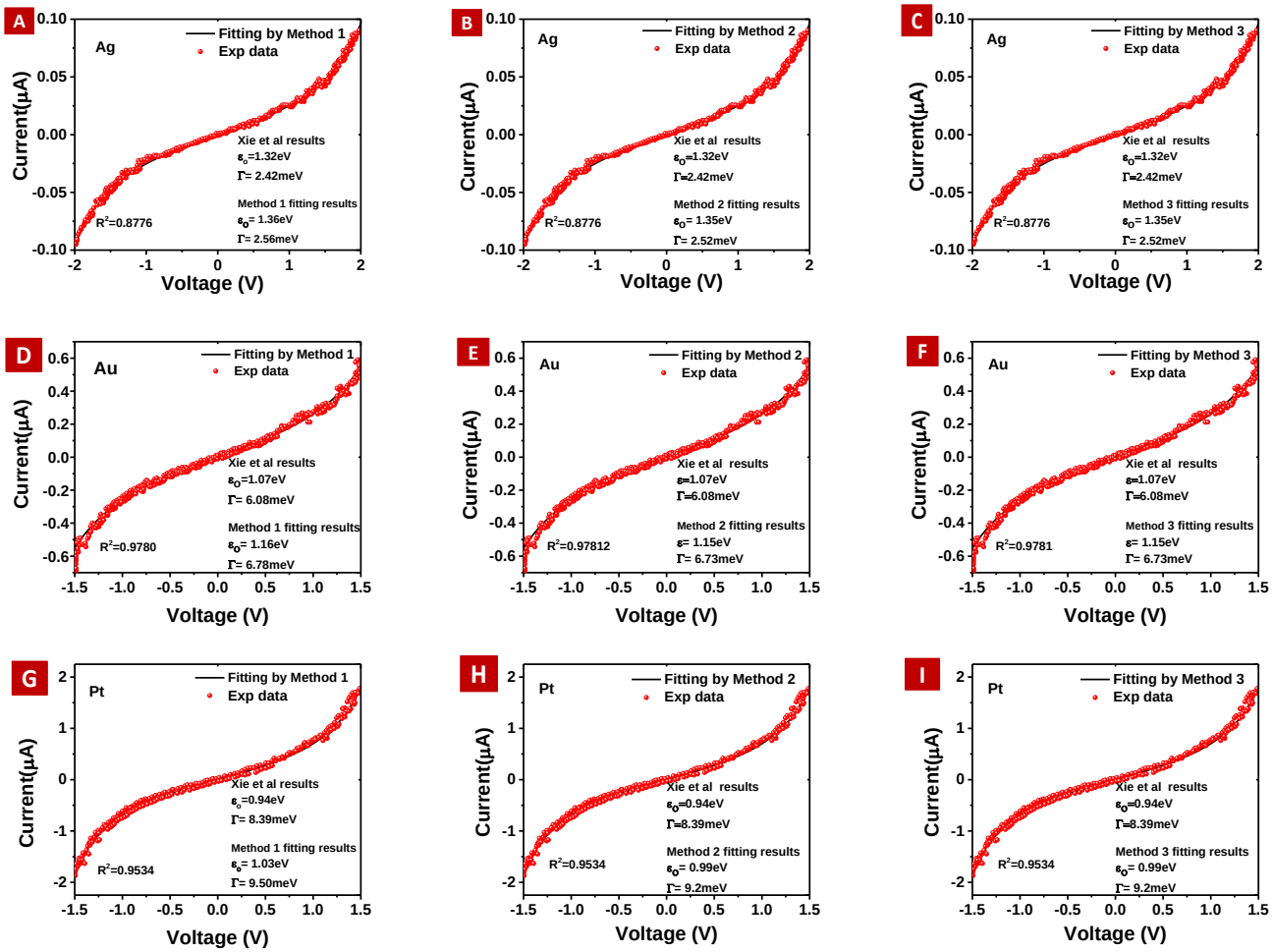

Fig S3: Current-Voltage Fitting plots of alkyl Dithiols, C10DT on Ag, Au, and Pt[1]

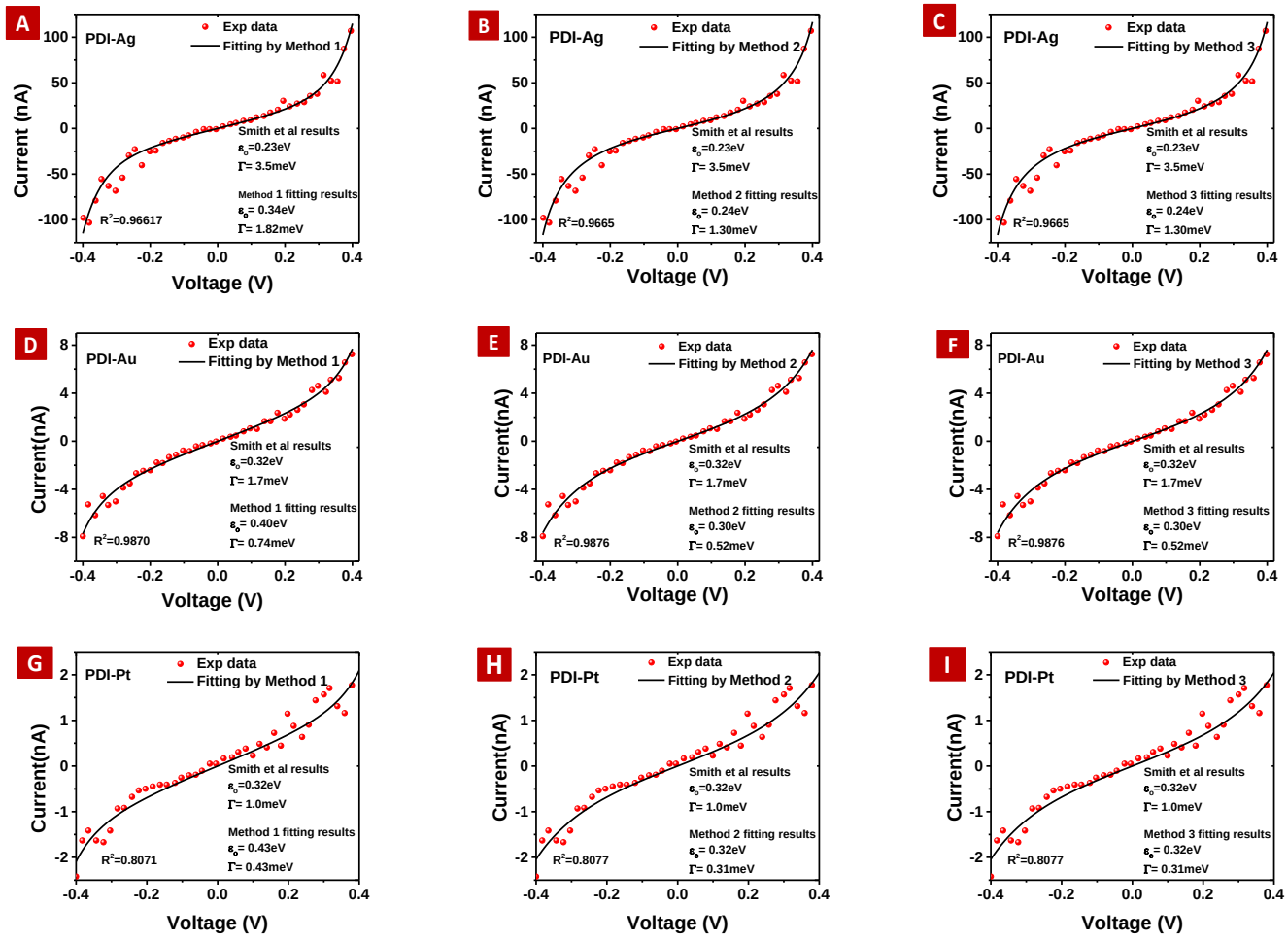

Fig S4: Current-Voltage Fitting plots of Isocyanide terminated perylene diimide (CN_2PDI) on Ag, Au, and Pt[2].

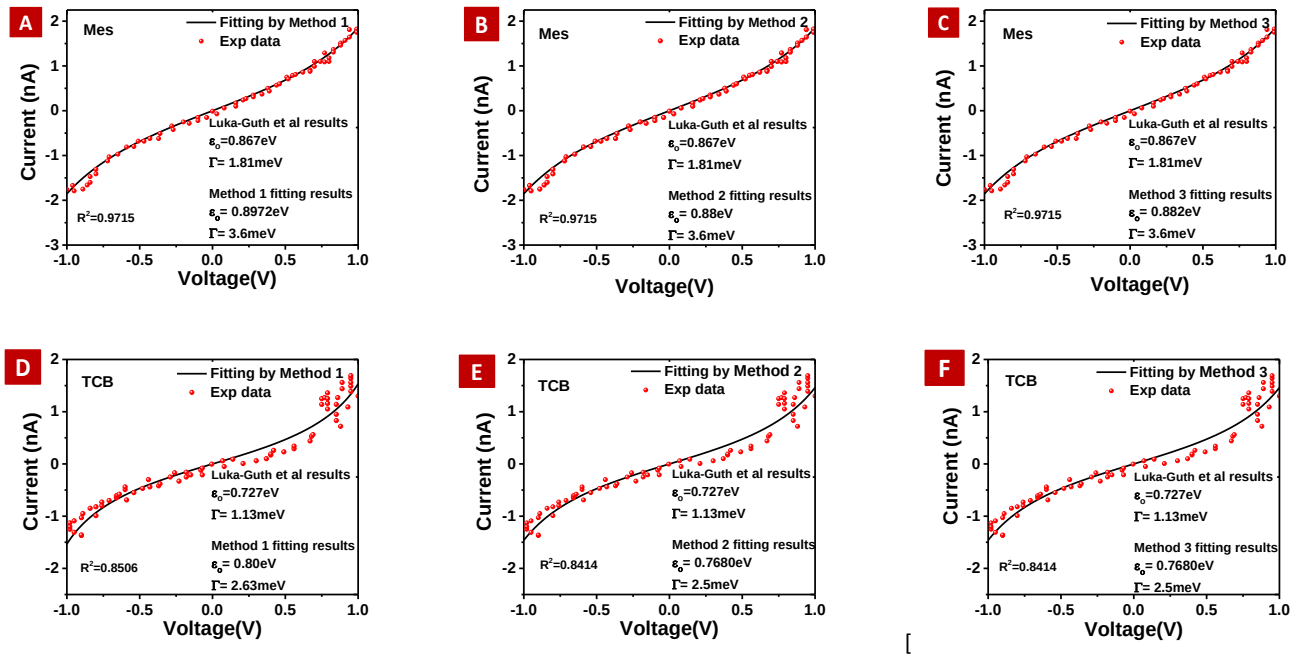

[

Fig S5: Current-Voltage Fitting plots of Mesitylene (Mes) and 1, 2, 4-trichlorobenzene (TCB)[3]

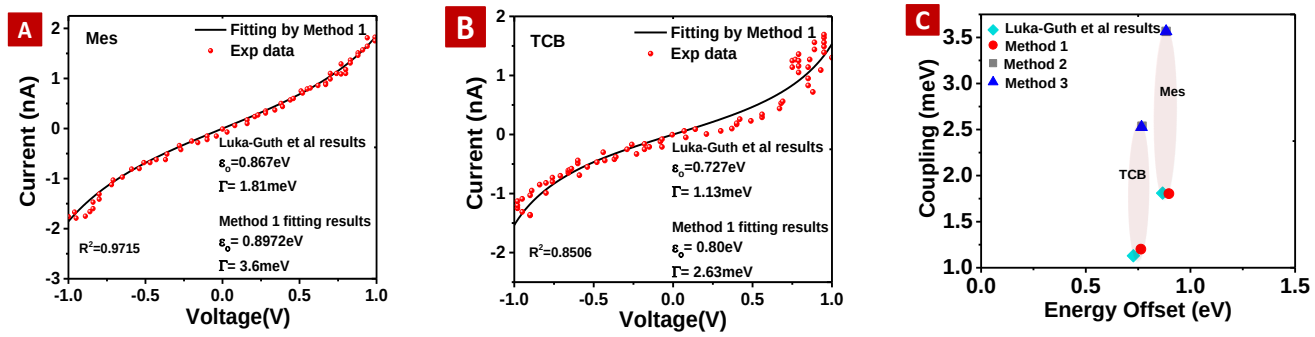

Fig S6: Current –Voltage and fitting plots of a). Mes, b). TCB molecular junctions from Luka-Guth et al reported results[3] using a big integration step (**0.032eV**) for Method 1. C). A comparison of the energy barrier and coupling obtained by fitting using three methods. Results for Method 1 are obtained from panel a, b and results for Method 2 and 3 are obtained in figure S5, B, E and C, F respectively)

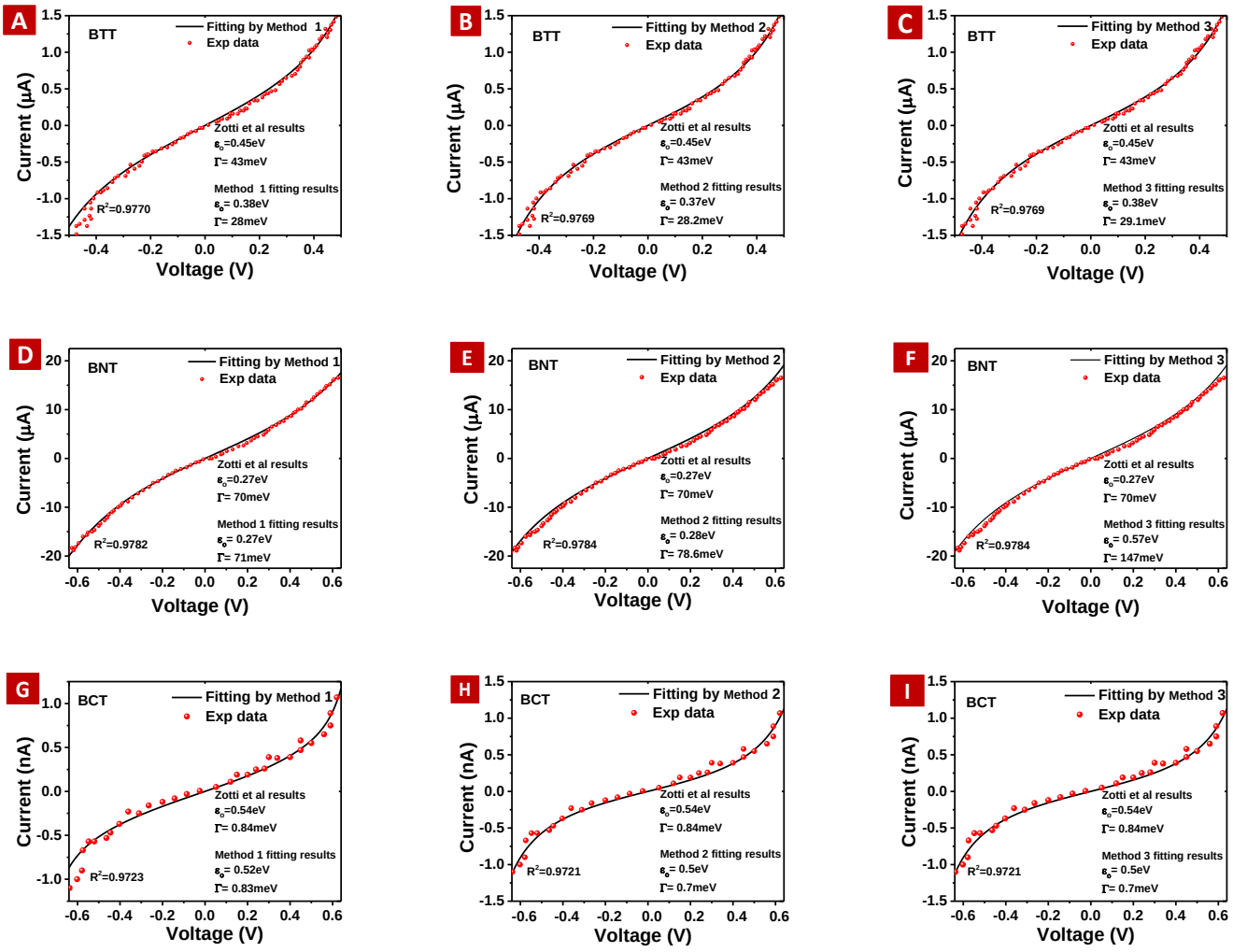

Fig S7: Current-Voltage Fitting plots of 4, 4-bisnitrotolane (BNT), 4, 4-bisthiotolane (BTT) and 4, 4-biscyanotolane (BCT) on Au[4]

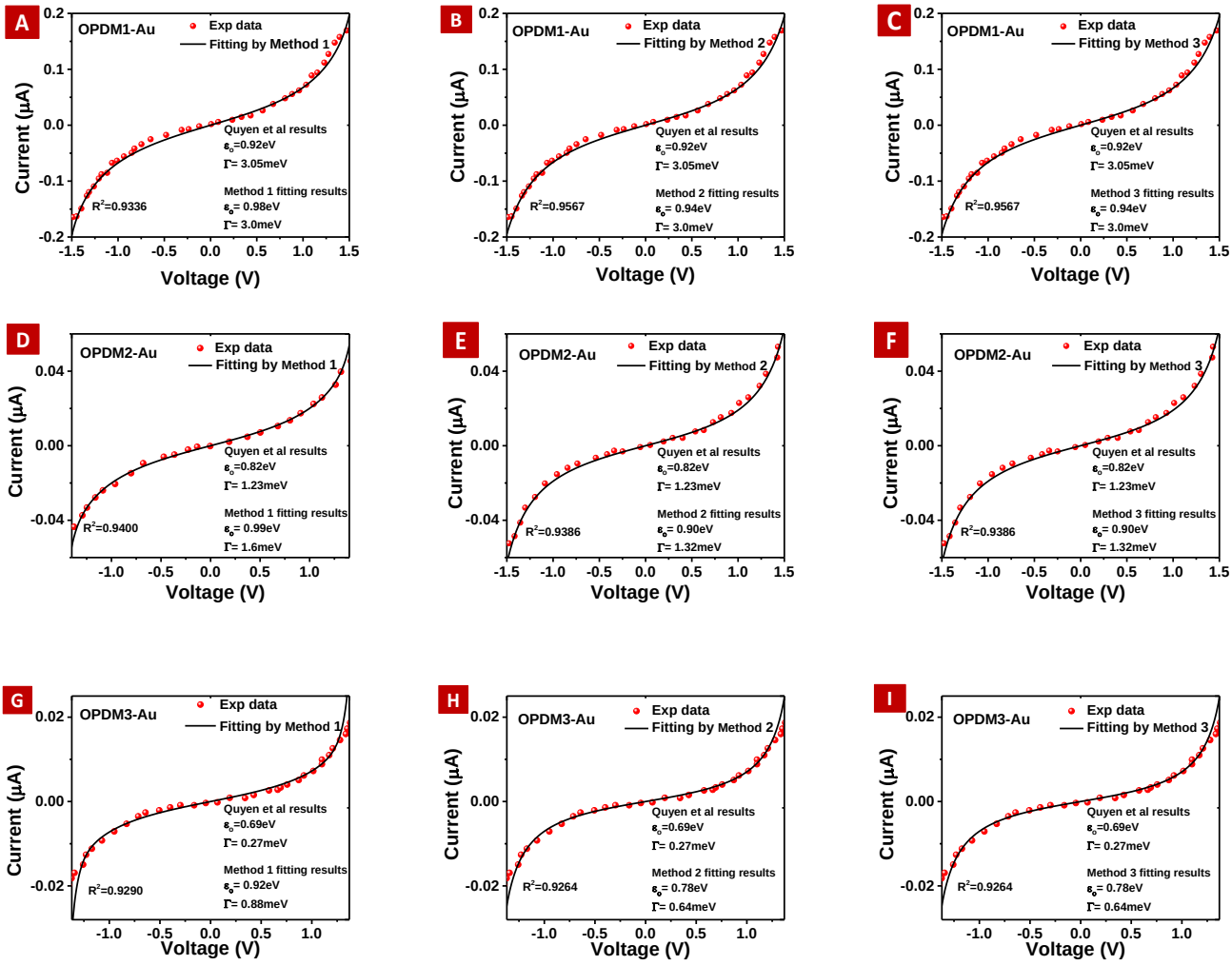

Fig S8: Current-Voltage Fitting plots of oligophenylene dimethanethiols (OPDMn) (n=1, 2 &3) on Au[5]

TEMPERATURE DEPENDENT TUNNELING TRANSPORT

Temperature dependence measurement in molecular junctions was often used to distinguish tunneling from hopping transport. Generally, it is believed that tunneling is temperature independent while hopping is temperature dependent. This is commonly true if we consider Method 2 and 3, where the Fermi distribution with temperature term was approximated into step function under the precondition that the thermal broadening of the Fermi distribution at room temperature (~25 meV) is relatively small in comparison to the coupling. However, on the other hand, when the coupling is weaker than the thermal broadening, tunneling can be temperature dependent, especially near resonance, i.e. small energy offset[6]. Low bias temperature dependence tunneling has been claimed in several studies.[2,7,8] For example, smith et al.[2] have experimentally demonstrated that isocyanide terminated perylene diimide (CN_2-PDI) molecular junction exhibit a low bias temperature dependent that could be attributed to broadening of the Fermi level. However, we would like to argue that the recognition of temperature dependent tunneling is actually quite vague. We use Method 1 to demonstrate the effect of thermal broadening at the Fermi level in tunneling transport since it encloses the temperature effect in Fermi function of the electrode. Based on the study of Smith et al, we applied two strategies. First, we extract the energy offset and coupling strength parameters by Method 1 based on their experimental result at 25 ℃, and then regenerate I-V curves using Method 1 at temperatures from 65 ℃ to -25 ℃ (figure S9A). In the second strategy, we generated I-V curves at different temperatures using Method 1 again (figure S9C), while this time, we used energy level and coupling parameter reported in their paper, which were obtained by fitting experimental results using Method 3. From the plots below, it can be seen that neither of them can reproduce their temperature dependent experimental results, which imply that the observed temperature dependent I-V behavior might not originate from the temperature dependent tunneling, or at least not pure single level based the temperature dependent tunneling. More study should be done to make this point clear in the future.

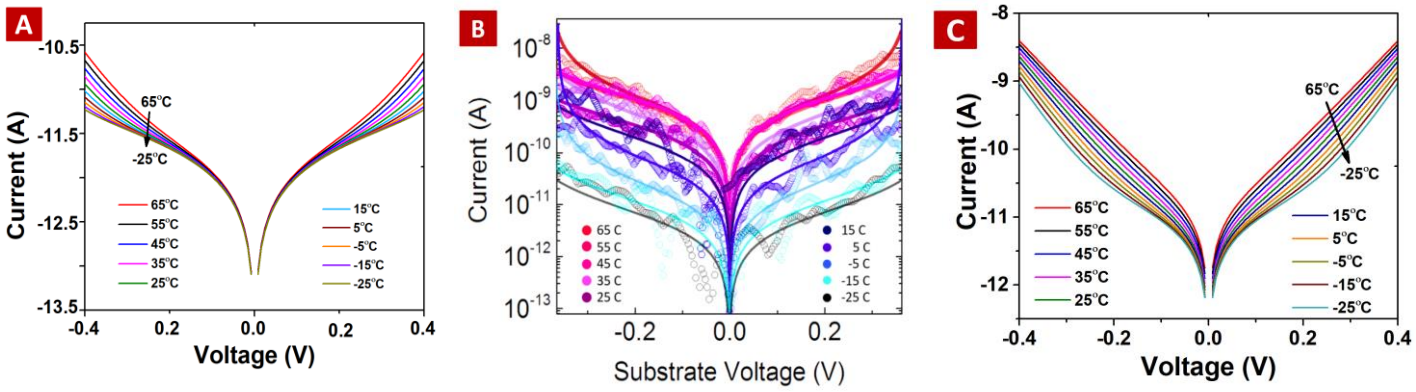

Figure S9: (A) & (C) Temperature dependent I-V curves generated from (Method 1), using ε_o and Γ obtained by re-fitting the experimental results CN_2-PDI on Pt (reprinted in panel B) from ref[2] by Method 1 (panel A), or using the ε_o and Γ provided in ref 2 (panel B).

The derivation of equation 2 (Method 2)

$I = \frac{2e^2}{h}\int_{-\infty}^{\infty} dE\ Tr(E)\ [f_L(E) - f_R(E)]$

Where the Fermi function is;

$f_{L,R}(E) = \frac{1}{1+\exp((E-\mu_{L,R})/kT))}$

At zero temperature

$\lim_{T\to 0} f_{L,R}(E) = \begin{cases} 0 & for\ E > \mu \\ 1 & for\ E < \mu \end{cases}$

The bias voltage can be introduced into the chemical potential in the Fermi function as $\mu_{L,R} = \mu_o \pm \frac{1}{2}\text{eV}$. Then at T=0

$$f_L(E) = \begin{cases} 0 & for\ E > \mu_o + \frac{1}{2}\text{eV} \\ 1 & for\ E < \mu_o + \frac{1}{2}\text{eV} \end{cases}$$

And

$$f_R(E) = \begin{cases} 0 & for\ E > \mu_o - \frac{1}{2}\text{eV} \\ 1 & for\ E < \mu_o - \frac{1}{2}\text{eV} \end{cases}$$

So, when incorporating these into the Landauer formula,

$$I = \frac{2e^2}{h}\int_{-\infty}^{\infty} dE\ Tr(E)\ [f_L(E) - f_R(E)]$$

$$= \frac{2e^2}{h}\int_{-\infty}^{\mu_o-\frac{1}{2}\text{eV}} dE\ Tr(E)\ [1-1] + \frac{2e^2}{h}\int_{\mu_o-\frac{1}{2}\text{eV}}^{\mu_o+\frac{1}{2}\text{eV}} dE\ Tr(E)\ [1-0]$$

$$+ \frac{2e^2}{h}\int_{\mu_o+\frac{1}{2}\text{eV}}^{\infty} dE\ Tr(E)\ [0-0] = \frac{2e^2}{h}\int_{\mu_o-\frac{1}{2}\text{eV}}^{\mu_o+\frac{1}{2}\text{eV}} dE\ Tr(E)$$

The above equation become

$$I = \frac{2e^2\Gamma_L\Gamma_{L_R}}{h}\int_{-\text{eV}/2}^{\text{eV}/2} \frac{1}{(E-\varepsilon_o)^2 + \frac{\Gamma^2}{2}}\ dE$$

Since the integration run assuming μ_o as the base 0 level and ε_o is the energy relative to μ_o

On integration the expression becomes;

$$I = \frac{4e^2}{h}\frac{\Gamma_L\Gamma_{L_R}}{\Gamma}\left[tan^{-1}\frac{E-\varepsilon_o}{\frac{\Gamma}{2}}\right]_{-eV/2}^{eV/2}$$

The final equation is; $I = \frac{4e^2}{h}\frac{\Gamma_L\Gamma_{L_R}}{\Gamma}\left(tan^{-1}\frac{\varepsilon_o+eV/2}{\frac{\Gamma}{2}} - tan^{-1}\frac{\varepsilon_o-eV/2}{\frac{\Gamma}{2}}\right)$

MATLAB CODE FOR NUMERICAL INTEGRATION AND FITTING

```
%%% Definition of fitting function
function IT=Tunneling1(beta,V)%Function

%%% Constant setting
e=1.60217e-19;% electron charge
h=6.62607004e-34;%Planks constant
hbar=h/(2*pi);

% below is the calculation of the I-V
G0=(2*e*e/hbar);% conductance quantum
kT=0.025; % at 298K RT
N=40 );% # of Molecules (Varies depending on junction)
IV=length(V);
Eg=beta(1);%energy offset
g1=beta(2);%coupling
g2=g1;
g=g2+g1;
alpha=0.5;%voltage division factor

 %Energy grid
NE=50001; ;% # of energy grid for numerical integration
E=linspace(-5,5,NE); );% energy grid for numerical
integration
dE=E(2)-E(1); );% energy step for numerical integration
D=(g/(2*pi))./((E.^2)+((g/2)^2));% Lorentzian Density of
states per eV
for iV=1:IV
Vd=V(iV);
UL=(alpha*Vd);%electrochemical potential
UL2=((1-alpha)*Vd);
f1=1./(1+exp((E-(Eg+UL))./kT));%Fermi function
f2=1./(1+exp((E-(Eg-UL2))./kT));
IT(iV)=((N*dE*G0*(sum(D.*(f1-
f2)))*(g1*g2/g)));%Tunneling equation
end

%Tunneling fitting
clear;
clc;
tdata=xlsread('folder');%import the data that used to fit
I=((tdata(:,2))); %current, notice the format of data
V=tdata:,1);
betaT0=['input Eg g'];    %Initial setting value for fitting
opts = statset('RobustWgtFun','bisquare','MaxIter',1000);%
Setting of the fitting algorithm
betaT=nlinfit(V,I,@Tunneling1,betaT0,opts); %fitting
function
EgT=betaT(1);       %fitting result of energy barrier
GamaR=betaT(2);      %fitting result of coupling strength
betaT1=[EgT GamaR];
VV=linspace(-2,2,501);     %fitting bias
Ifit=Tunneling1(betaT1,VV);% fitting result of current
figure(1)
plot(VV,Ifit,'b')% plot the I-V of fitting results
hold on
plot(V,I,'r.')% plot the  I-V of imported data
xlabel('Voltage(v)')
ylabel('Current(A)')
title('Current---Voltage')
grid on
```

References

1. Z. Xie, I. Baldea and C. D. Frisbie, *J. Am. Chem. Soc.*, 2019, **141**, 18182-18192.
2. C. E. Smith, Z. Xie, I. Baldea and C. D. Frisbie, *Nanoscale.*, 2018, **10**, 964-975.
3. K. Luka-Guth, S. Hambsch, A. Bloch, P. Ehrenreich, B. M. Briechle, F. Kilibarda, T. Sendler, D. Sysoiev, T. Huhn, A. Erbe and E. Scheer, *Beilstein J. Nanotechnol*, 2016, **7**, 1055–1067.
4. L. A. Zotti, T. Kirchner, J. C. Cuevas, F. Pauly, T. Huhn, E. Scheer and A. Erbe, *Small.*, 2010, **6**, 1529-1535.
5. Q. V. Nguyen, Z. Xie and C. D. Frisbie, *J. Phys. Chem. C.*, 2021, **125**, 4292−4298.
6. I. Baldea, *Organic Electronics* 2017, **49**, 19-23.
7. C. Jia, A. Migliore, N. Xin, S. Huang, J. Wang, Q. Yang, S. Wang, H. Chen, D. Wang, B. Feng, Z. Liu, G. Zhang, D.-H. Qu, H. Tian, M. A. Ratner, H. Q. Xu, A. Nitzan and X. Guo, *Science*, 2016, **352**, 1443-1445.
8. M. Kamenetsk, J. R. Widawsky, M. Dell'Angela, M. Frei and L. Venkataraman, *Chem. Phys.* , 2017, **146**, 092311.